JOURNAL OF GUIDANCE, CONTROL, AND DYNAMICS
Vol. 27, No. 5, September–October 2004

Periodic H_2 Synthesis for Spacecraft Attitude Control with Magnetorquers

Rafal Wiśniewski* and Jakob Stoustrup†
Aalborg University, DK-9220 Aalborg East, Denmark

A control synthesis for a spacecraft equipped with a set of magnetorquer coils is addressed. The electromagnetic actuation is particularly attractive for small low-cost spacecraft missions, due to their relatively low price, high reliability, light weight, and low power consumption. The interaction between the Earth's magnetic field and an artificial magnetic field generated by the coils produces a control torque. The magnetic attitude control is intrinsically periodic due to cyclic variation of the geomagnetic field in orbit. The control performance is specified by the generalized H_2 operator norm. A linear matrix inequality-based algorithm is proposed for attitude control synthesis. Simulation results are provided, showing the prospect of the concept for onboard implementation.

Nomenclature

$\boldsymbol{b}$	=	local geomagnetic field vector
$\boldsymbol{I}$	=	identity matrix
im$\boldsymbol{A}$	=	image of A
$\boldsymbol{J}$	=	moments of inertia tensor
J_x, J_y, J_z	=	moments of inertia about x, y, and z principal axes
ker$\boldsymbol{A}$	=	null space of A
l_2	=	space of all sequences $\boldsymbol{u}$ such that $\|\boldsymbol{u}\| < \infty$
$\mathbb{R}^{m \times p}$	=	all m by p matrices with real entries
$S(\mathbb{R}^{n \times n})$	=	all symmetric n by n matrices with real entries
tr$\boldsymbol{A}$	=	trace of $\boldsymbol{A}$
$\lvert \cdot \rvert$	=	Euclidean norm
$\lVert \cdot \rVert$	=	l_2 norm
$\lVert \cdot \rVert_2$	=	H_2 norm
$\mathbb{Z}_+$	=	set of all positive integers and zero

I. Introduction

THE tremendous progress in microelectronics in the past two decades has made small, inexpensive spacecraft missions very attractive and technologically viable. However, due to reduced allocated mission cost and limited space available in a satellite, onboard actuators are often very simple. A typical choice is a set of magnetorquer coils. The interaction of the geomagnetic field and artificially generated field in the coils produces a control torque. The attitude control scheme developed in this paper uses the observation that the external magnetic field is periodic. Indeed, the time propagation of the geomagnetic field observed from an Earth-stabilized spacecraft is a superposition of two periodic motions: orbital and the Earth spin. If the ratio of the two periods is a rational number, the geomagnetic field observation is periodic. A concept for attitude control based on electromagnetic actuation has gained considerable attention lately. Early work was based on an idea of designing a magnetic controller for the system with averaged parameters, rather than time varying parameters. This design strategy was used both for bias momentum satellites[1–3] and three-axis control.[4] In recent papers, more sophisticated control schemes were proposed, where not only linear[5–9] but also nonlinear control methods[10–13] were studied. In this paper, the spacecraft is considered as a discrete linear periodic system and the H_2 control synthesis problem is solved. The optimization problem is formulated in this work by certain linear matrix inequalities (LMI).

Previous studies have shown that periodic systems are similar to the linear time-invariant ones. The stability, for instance, is determined by the eigenvalues of the transition matrix computed for one period. Likewise stationary solutions to Lyapunov and Riccati equations play fundamental roles in the stability analysis. These similarities are explained by a lift operator that replaces a periodic system with a time-invariant counterpart. Despite this resemblance, the control synthesis seems to be less straightforward because a causal control has to obey a certain Toeplitz structure condition. Illustrative of this problem is that the use of standard control design algorithms for linear-time invariant systems may result in a noncausal controller for a lifted system.

A broad spectrum of results for periodic systems are available in the literature. The topics of structural properties, stability, quadratic optimal control, and their relations to the periodic Lyapunov and Riccati equations were reported in Refs. 14–18. An impetus for development was the introduction of the lift operator.[19] As the results known from control theory of linear time-invariant systems became generalized to periodic systems, the techniques such as pole placement,[20] linear quadratic,[15] and H_∞ control[21] became available for periodic systems. Despite the maturity of the field, only recently has work on robust stability for periodic systems been published.[22,23] A considerable step forward has been taken in Ref. 24. The authors related the periodic systems to the LMI technique and solved the H_∞ synthesis problem.

The contribution of this study is an LMI formulation of the H_2 control synthesis problem. The paper considers a periodic discrete time system, for which the performance is specified by the generalized H_2 operator norm.[25] The generalized norm is related to the periodic solution of a certain Lyapunov equation. Then the sufficient and necessary conditions for solvability of a suboptimal control synthesis problem are formulated. The proof provided in this paper is similar to the LTI case.[26] It is constructive; thereby, it provides an algorithm for state feedback control synthesis.The result of this paper can be considered as a variation of the H_2 control synthesis for linear discrete time-invariant systems[27,28] to periodic processes.

The outcome of this work is an algorithm for state feedback synthesis of a spacecraft on a highly inclined low Earth orbit. It appears that the complexity of the resulting algorithm is considerable. However, the computational burden of the control synthesis is in the off-line calculation, whereas the onboard algorithm is simple.

To begin, some properties of the periodic systems, as stability,the notion of the lift operator, and the periodic Lyapunov equation, are briefly recalled in Sec. II. The system performance is specified by the H_2 norm generalized for periodic systems in Sec. III. In the next step, the periodic control design is converted to a solution of LMIs. The main result is a formulation of conditions for solvability

Received 31 January 2003; accepted for publication 12 April 2004.

*Associate Professor, Department of Control Engineering, Fredrik Bajers Vej 7C; raf@control.aau.dk.

†Professor, Department of Control Engineering, Fredrik Bajers Vej 7C; jakob@control.aau.dk.

of the periodic H_2 control. This is the subject of Sec. IV. The proof, postponed to the Appendix, is constructive and gives rise to an algorithm for controller synthesis. The findings are implemented on a model of a low-Earth-orbit spacecraft in Sec. V and validated in a simulation study in Sec. VI.

II. Properties of Periodic Systems

It is assumed throughout that full state information is available, either directly via measurements or by state observation. The argument for using the latter paradigm is that the separation principle is valid for periodic systems.[29]

Consider a discrete signal $\boldsymbol{u} = \{\boldsymbol{u}(t)\},\ t \in \mathbb{Z}_+$, where $\boldsymbol{u}(t) \in \mathbb{R}^m$. The space of all sequences $\boldsymbol{u}$ such that

$$\|\boldsymbol{u}\|^2 \equiv \sum_{t\in\mathbb{Z}_+} \boldsymbol{u}(t)^T \boldsymbol{u}(t) < \infty$$

is denoted by l_2^m. We shall study a discrete time-linear periodic system $S_o : (l_2)^{s+m} \to (l_2)^{r+p}$, $(\boldsymbol{w}, \boldsymbol{u}) \mapsto (\boldsymbol{z}, \boldsymbol{y})$ as follows with control input $\boldsymbol{u}$, the measurement $\boldsymbol{y}$, an exogenous input $\boldsymbol{w}$, and an exogenous output $\boldsymbol{z}$. The last two signals are used for performance specification, and they need to be neither the actual input nor output to the system:

$$\begin{aligned}\boldsymbol{x}(t+1) &= \boldsymbol{A}(t)\boldsymbol{x}(t) + \boldsymbol{B}_1(t)\boldsymbol{w}(t) + \boldsymbol{B}_2(t)\boldsymbol{u}(t)\\ \boldsymbol{z}(t) &= \boldsymbol{C}_1(t)\boldsymbol{x}(t) + \boldsymbol{D}_{12}(t)\boldsymbol{u}(t)\\ \boldsymbol{y}(t) &= \boldsymbol{C}_2(t)\boldsymbol{x}(t) + \boldsymbol{D}_{21}(t)\boldsymbol{w}(t)\end{aligned} \tag{1}$$

The functions $\boldsymbol{A} : \mathbb{Z}_+ \to \mathbb{R}^{n\times n}$, $\boldsymbol{B}_1 : \mathbb{Z}_+ \to \mathbb{R}^{n\times s}$, $\boldsymbol{B}_2 : \mathbb{Z}_+ \to \mathbb{R}^{n\times m}$, $\boldsymbol{C}_1 : \mathbb{Z}_+ \to \mathbb{R}^{r\times n}$, $\boldsymbol{C}_2 : \mathbb{Z}_+ \to \mathbb{R}^{p\times n}$, $\boldsymbol{D}_{12} : \mathbb{Z}_+ \to \mathbb{R}^{r\times m}$, and $\boldsymbol{D}_{21} : \mathbb{Z}_+ \to \mathbb{R}^{p\times s}$ are continuous and N periodic. Recall that a function $A : \mathbb{Z}_+ \to \mathbb{R}^{n\times n}$ is N periodic if $\boldsymbol{A}(t+N) = \boldsymbol{A}(t)$.

Full state information has been assumed, which gives rise to particularly simple matrices $\boldsymbol{C}_2$ and $\boldsymbol{D}_{21}$: $\boldsymbol{C}_2 = I$ and $\boldsymbol{D}_{21} = 0$. It follows that the state feedback $\boldsymbol{u}(t) = \boldsymbol{K}(t)\boldsymbol{x}(t), \boldsymbol{K} : \mathbb{Z}_+ \to \mathbb{R}^{m\times n}$ can be employed. The objective of the control design in this work is to compute an N-periodic gain $\boldsymbol{K}$ for which the transfer function $S_c : (l_2)^s \to (l_2)^r,\ \boldsymbol{w} \mapsto \boldsymbol{z}$,

$$\begin{aligned}\boldsymbol{x}(t+1) &= \boldsymbol{A}_c(t)\boldsymbol{x}(t) + \boldsymbol{B}_1(t)\boldsymbol{w}(t)\\ \boldsymbol{z}(t) &= \boldsymbol{C}_c(t)\boldsymbol{x}(t)\end{aligned} \tag{2}$$

where $\boldsymbol{A}_c = \boldsymbol{A} + \boldsymbol{B}_2\boldsymbol{K}$ and $\boldsymbol{C}_c = \boldsymbol{C}_1 + \boldsymbol{D}_{12}\boldsymbol{K}$ are stable and satisfy a certain performance specification.

It will be crucial in the next section to establish a relation between stability of a periodic system and a solution of the periodic Lyapunov equation. The following theorem states sufficient and necessary conditions for a periodic system to be stable[15]:

Theorem 1: A system $\boldsymbol{A}(t)$ is stable if and only if, for any periodic $\boldsymbol{R}(t)$ such that $(\boldsymbol{A}(t), \boldsymbol{R}(t))$ is detectable there exists a symmetric, periodic, positive semidefinite solution $\boldsymbol{Q}(t)$ of the following periodic Lyapunov equation:

$$\boldsymbol{Q}(t-1) = \boldsymbol{A}(t)^T\boldsymbol{Q}(t)\boldsymbol{A}(t) + \boldsymbol{R}(t)^T\boldsymbol{R}(t), \qquad t \in \mathbb{Z} \tag{3}$$

When exponentially stable A is assumed, the solution to Eq. (3) is bounded and given by the following formula[30]:

$$\boldsymbol{Q}(t) = \sum_{j=t+1}^{\infty} \Phi(j, t+1)^T \boldsymbol{R}(j)^T \boldsymbol{R}(j) \Phi(j, t+1) \tag{4}$$

where $\boldsymbol{\Phi}(t, t_0)$ is the state transition matrix at sample t with the initial time t_0, that is, $\Phi(t, t_0) = \boldsymbol{A}(t-1)\boldsymbol{A}(t-2), \ldots, \boldsymbol{A}(t_0)$.

The last topic addressed in this section is a lift operator.[19] It is an isomorphism that takes a linear periodic system into a time-invariant counterpart. It suffices in this work to leave out the development; it is derived explicitly by listing all of the outputs of an N-periodic system at time instances t to $t+N-1$. Particularly, for the system S_c in Eq. (2) one has

$$\begin{aligned}\boldsymbol{x}(t+N) &= \bar{\boldsymbol{A}}\boldsymbol{x}(t) + \bar{\boldsymbol{B}}_1\boldsymbol{w}(t) + \bar{\boldsymbol{B}}_2\boldsymbol{w}(t+1) + \cdots\\ &\quad + \bar{\boldsymbol{B}}_N\boldsymbol{w}(t+N-1)\\ \boldsymbol{y}(t) &= \bar{\boldsymbol{C}}_N\boldsymbol{x}(t)\\ &\ \ \vdots\\ \boldsymbol{y}(t+i) &= \bar{\boldsymbol{C}}_{N-i}\boldsymbol{x}(t) + \bar{\boldsymbol{D}}_{i+1,1}\boldsymbol{w}(t) + \cdots + \bar{\boldsymbol{D}}_{i+1,i}\boldsymbol{w}(t+i-1)\\ &\ \ \cdots\\ \boldsymbol{y}(t+N-1) &= \bar{\boldsymbol{C}}_1\boldsymbol{x}(t) + \bar{\boldsymbol{D}}_{N,1}\boldsymbol{w}(t) + \cdots + \bar{\boldsymbol{D}}_{N,N-1}\boldsymbol{w}(t+N-2)\end{aligned} \tag{5}$$

where

$$\begin{aligned}\bar{\boldsymbol{A}} &= \boldsymbol{\Phi}(t+N, t) = \boldsymbol{A}_c(t+N-1), \ldots, \boldsymbol{A}_c(t)\\ \bar{\boldsymbol{B}}_k(t) &= \boldsymbol{\Phi}(t+N, t+k)\boldsymbol{B}_1(t+k-1)\\ \bar{\boldsymbol{C}}_k(t) &= \boldsymbol{C}_c(t+N-k)\boldsymbol{\Phi}(t+N-k, t)\\ \bar{\boldsymbol{D}}_{k,j}(t) &= \boldsymbol{C}_c(t+k-1)\boldsymbol{\Phi}(t+k-1, t+j)\boldsymbol{B}_1(t+j-1)\end{aligned}$$

Notice that the matrix $\bar{\boldsymbol{A}}$ is the monodromy matrix of the Floquet theory (see Ref. 16). The monodromy matrix is time independent, and its eigenvalues in the open unit disk determine the stability of the system.

The result of gathering all of the inputs $\boldsymbol{w}(t), \ldots, \boldsymbol{w}(t+N-1)$ into an input vector $\boldsymbol{\xi}(t)$ and all of the outputs into a single output vector $\boldsymbol{\psi}(t)$ is the following time-invariant system $\bar{S}_c : (l_2)^{sN} \to (l_2)^{rN},\ \boldsymbol{\xi} \mapsto \boldsymbol{\psi}$,

$$\begin{aligned}\boldsymbol{x}(t+N) &= \bar{\boldsymbol{A}}\boldsymbol{x}(t) + \bar{\boldsymbol{B}}\boldsymbol{\xi}(t)\\ \boldsymbol{\psi}(t) &= \bar{\boldsymbol{C}}\boldsymbol{x}(t) + \bar{\boldsymbol{D}}\boldsymbol{\xi}(t)\end{aligned} \tag{6}$$

where

$$\bar{\boldsymbol{B}} = [\bar{\boldsymbol{B}}_1 \quad \bar{\boldsymbol{B}}_2 \quad \ldots \quad \bar{\boldsymbol{B}}_N,], \qquad \begin{bmatrix}\bar{\boldsymbol{C}}_N\\ \bar{\boldsymbol{C}}_{N-1}\\ \vdots\\ \bar{\boldsymbol{C}}_1\end{bmatrix}$$

$$\bar{\boldsymbol{D}} = \begin{bmatrix} 0 & 0 & \ldots & 0 & 0\\ \bar{\boldsymbol{D}}_{2,1} & 0 & \ldots & 0 & 0\\ \vdots & \ddots & & & \\ \bar{\boldsymbol{D}}_{N-1,1} & \ldots & \bar{\boldsymbol{D}}_{N-1,N-2} & 0 & 0\\ \bar{\boldsymbol{D}}_{N,1} & \bar{\boldsymbol{D}}_{N,2} & \ldots & \bar{\boldsymbol{D}}_{N,N-1} & 0\end{bmatrix}$$

We shall call the system $\bar{S}_c$ the lift of S_c.

III. Performance Specification

The H_2 operator norm for a discrete, time-invariant, stable, causal system $R : (H_2)^m \to (H_2)^p$ is defined[31] by

$$\|R\|_2 \equiv \left(\frac{1}{2\pi}\mathrm{tr}\int_{-\pi}^{\pi} R(e^{i\tau})R^*(e^{i\tau})\,\mathrm{d}\tau\right)^{\frac{1}{2}} \tag{7}$$

where tr stands for the trace of a matrix. Equivalently by Parseval's relation between the time and frequency domains, the H_2 operator norm is

$$\|R\|_2 = \|r\|_2 \equiv \left[\sum_{i=1}^{m} \|r\delta(t)e_i\|^2\right]^{\frac{1}{2}} \tag{8}$$

where $r: (l_2)^m \to (l_2)^p$ and e_i is the standard basis of the input space $\mathbb{R}^m$; thus, δe_i is the impulse applied to the ith input. To illustrate definition (8), we shall compute the H_2 norm for the system $\bar{S}_c$. Notice that $\bar{S}_c$ is the lift of S_c', thus, it is time invariant,

$$\|\bar{S}_c\|_2 = \mathrm{tr} \sum_{i \in \mathbb{Z}_+} \bar{\boldsymbol{B}}^T (\bar{\boldsymbol{A}}^i)^T \bar{\boldsymbol{C}}^T \bar{\boldsymbol{C}} \bar{\boldsymbol{A}}^i \bar{\boldsymbol{B}} + \mathrm{tr} \bar{\boldsymbol{D}}^T \bar{\boldsymbol{D}} \tag{9}$$

The preceding definition indicates that the H_2 norm is characterized by the l_2 norm of the impulse response; on the other hand, the response of a periodic system is dependent on the time when the impulse signal is initiated. Following Ref. 25, a generalized H_2 norm for the periodic system S_c is an integration of Eq. (8) within one period:

$$\|S_c\|_2 \equiv \left[\frac{1}{N} \sum_{j=0}^{N-1} \sum_{k=1}^{m} \|S_c \delta(t-j) e_k\|^2 \right]^{\frac{1}{2}} \tag{10}$$

The definition in Eq. (10) corresponds to the standard H_2 norm if the system S_c were time invariant. Observe also that the l_2 norm in Eq. (10) can be written as

$$\|S_c \delta(t-j) e_k\| = \|\bar{S}_c \delta(t) e_{k+sj}\| \tag{11}$$

where s is the number of inputs to the periodic system S_c. Thus, the H_2 norm for a periodic system is equivalent to $1/\sqrt{N}$ of the H_2 norm of its lift.

When Eqs. (9–10) are used, the generalized H_2 norm for the system S_c takes the following form:

$$\|S_c\|_2 = \frac{1}{\sqrt{N}} \|\bar{S}_c\|_2 = \left(\frac{1}{N} \mathrm{tr} \sum_{i \in \mathbb{Z}_+} \begin{bmatrix} \boldsymbol{B}_1(0)^T \boldsymbol{\Phi}(N,1)^T \\ \boldsymbol{B}_1(1)^T \boldsymbol{\Phi}(N,2)^T \\ \cdots \\ \boldsymbol{B}_1(N-1)^T \end{bmatrix} \boldsymbol{\Phi}^i(N,0)^T \left[\boldsymbol{\Phi}(N-1,0)^T \boldsymbol{C}_c(N-1)^T \quad \boldsymbol{\Phi}(N-2,0)^T \boldsymbol{C}_c(N-2)^T \quad \cdots \quad \boldsymbol{C}_c(0)^T \right]^T \right.$$
$$\left. \times \begin{bmatrix} \boldsymbol{C}_c(N-1)\boldsymbol{\Phi}(N-1,0) \\ \boldsymbol{C}_c(N-2)\boldsymbol{\Phi}(N-2,0) \\ \cdots \\ \boldsymbol{C}_c(0) \end{bmatrix} \boldsymbol{\Phi}(N,0) \left[\boldsymbol{\Phi}(N,1)\boldsymbol{B}_1(0) \quad \boldsymbol{\Phi}(N,2)\boldsymbol{B}_1(1) \quad \cdots \quad \boldsymbol{B}_1(N-1) \right] \right)^{\frac{1}{2}} \tag{12}$$

where $\boldsymbol{\Phi}(j,k) = \boldsymbol{A}_c(j-1), \ldots, \boldsymbol{A}_c(k+1)\boldsymbol{A}_c(k)$. When the terms containing matrix $\boldsymbol{B}_1(\cdot)$ are grouped, Eq. (12) is simplified to the following form:

$$\|S_c\|_2 = \left(\frac{1}{N} \mathrm{tr} \sum_{t=0}^{N-1} \boldsymbol{B}_1(t)^T \times \left[\sum_{j=t+1}^{\infty} \boldsymbol{\Phi}(j,t+1)^T \boldsymbol{C}_c(j)^T \boldsymbol{C}_c(j) \boldsymbol{\Phi}(j,t+1) \right] \boldsymbol{B}_1(t) \right)^{\frac{1}{2}} \tag{13}$$

The expression in the brackets is, by (4), the solution of the following Lyapunov equation

$$\boldsymbol{Q}(t-1) = \boldsymbol{A}_c(t)^T \boldsymbol{Q}(t) \boldsymbol{A}_c(t) + \boldsymbol{C}_c(t)^T \boldsymbol{C}_c(t) \tag{14}$$

hence, the H_2 operator norm can be written

$$\|S_c\|_2 = \left[\frac{1}{N} \mathrm{tr} \sum_{t=0}^{N-1} \boldsymbol{B}_1(t)^T \boldsymbol{Q}(t) \boldsymbol{B}_1(t) \right]^{\frac{1}{2}} \tag{15}$$

where $\boldsymbol{Q}: \mathbb{Z}_+ \to S(\mathbb{R}^{n \times n})$ is the periodic solution of Eq. (14).

Here in after, Eq. (15) will be regarded as an equivalent definition of the H_2 operator norm. It will be applied to express the desired performance of a controller.

IV. Control Synthesis

The objective of the design is to find a controller such that the closed-loop system has the generalized H_2 norm smaller than some possibly small constant γ. In other words, we want to compute a periodic control $\boldsymbol{K}$ such that the system S_c satisfies

$$\|S_c\|_2 < \gamma \tag{16}$$

This paradigm is traditionally called the suboptimal control problem. Note that it is different from the optimal design, which finds the control with the smallest possible norm. A closed-loop system satisfying inequality (16) and being $(\boldsymbol{A}_c, \boldsymbol{C}_c)$ detectable is stable by Theorem 1.

The next challenge is to determine the prerequisites for solvability of the suboptimal H_2 problem. The immediate one is stabilizability of $(\boldsymbol{A}, \boldsymbol{B}_2)$. The next theorem states necessary and sufficient conditions for H_2 suboptimal problem by a number of LMIs.

Theorem 2: Consider a periodic discrete time system S_c, for which $(\boldsymbol{A}, \boldsymbol{B}_2)$ is stabilizable. The suboptimal H_2 problem (16) is solvable if and only if there exists an N-periodic function $Q: \mathbb{Z}_+ \to S(\mathbb{R}^{n \times n})$ and N-periodic function $Z: \mathbb{Z}_+ \to \mathbb{R}^{s \times s}$ such that for all $t = 1, \ldots, N$ the following LMIs are satisfied:

$$\left[\boldsymbol{W}_1(t)^T A(t) + \boldsymbol{W}_2(t)^T \boldsymbol{C}_1(t)\right] \boldsymbol{Q}(t-1) \left[\boldsymbol{A}(t)^T \boldsymbol{W}_1(t) + \boldsymbol{C}_1(t)^T \boldsymbol{W}_2(t)\right] - \boldsymbol{W}_1(t)^T \boldsymbol{Q}(t) \boldsymbol{W}_1(t) - \boldsymbol{W}_2(t)^T \boldsymbol{W}_2(t) < 0 \tag{17}$$

$$\begin{bmatrix} \boldsymbol{Q}(t) & \boldsymbol{B}_1(t) \\ \boldsymbol{B}_1(t)^T & \boldsymbol{Z}(t) \end{bmatrix} > 0 \tag{18}$$

$$\mathrm{tr}\left[\sum_{t=0}^{N-1} \boldsymbol{Z}(t) \right] < N\gamma^2 \tag{19}$$

where

$$\mathrm{im} \begin{bmatrix} \boldsymbol{W}_1(t) \\ \boldsymbol{W}_2(t) \end{bmatrix} = \ker\left[\boldsymbol{B}_2(t)^T \quad \boldsymbol{D}_{12}(t)^T \right]$$

For clarity, the proof of Theorem 2 will be deferred to the Appendix. In the proof, the H_2 control synthesis is decomposed into a feasibility problem consisting of finding $\boldsymbol{Q}$ and $\boldsymbol{Z}$ meeting the inequalities (17–19) and a problem of finding a periodic control gain $\boldsymbol{K}$ satisfying the following LMI for all $t = 1, \ldots, N$,

$$\begin{bmatrix} -\boldsymbol{Q}(t) & \boldsymbol{A}(t) & 0 \\ \boldsymbol{A}(t)^T & -\boldsymbol{Q}^{-1}(t-1) & \boldsymbol{C}_1(t)^T \\ 0 & \boldsymbol{C}_1(t) & -\boldsymbol{I} \end{bmatrix} + \left[\boldsymbol{B}_2(t)^T \quad 0 \quad \boldsymbol{D}_{12}(t)^T \right]^T \boldsymbol{K}(t) \times [0 \quad \boldsymbol{I} \quad 0] + [0 \quad \boldsymbol{I} \quad 0]^T \boldsymbol{K}(t)^T \left[\boldsymbol{B}_2(t)^T \quad 0 \quad \boldsymbol{D}_{12}(t)^T \right] < 0 \tag{20}$$

The proof of Theorem 2 is constructive and leads to the following design algorithm.

Algorithm:

1) For each $t = 1, \ldots, N$ find a symmetric matrix $\boldsymbol{Q}(t)$ and a matrix $\boldsymbol{Z}(t)$ satisfying LMIs (17–19).

2) For each $t = 1, \ldots, N$ compute a matrix $\boldsymbol{K}(t)$, which satisfies LMI (20).

This algorithm will be used in Sec. V for the periodic state feedback synthesis.

Remark: A time-invariant control gain is often desirable for a simple onboard implementation of the attitude control system. In this case, a periodic function $\boldsymbol{K} : \mathbb{Z}_+ \to \mathbb{R}^{m \times n}$ in step 2 is treated as constant, $\boldsymbol{K} \in \mathbb{R}^{m \times n}$. The resulting control is stable; however, the matrix $\boldsymbol{K}$ does not correspond in general to the optimal solution.

This remark sounds innocent: however, it has an impact on application in magnetic control. It gives an algorithm for automatic design of a constant gain magnetic control discussed in Refs. 2–4.

This section is concluded by giving a hint on a choice of the weight matrices $\boldsymbol{C}_1$, $\boldsymbol{D}_{12}$, and $\boldsymbol{B}_1$. Equation (1) shows that the matrix $\boldsymbol{B}_1$ specifies the channel and the amplitude of the external disturbances. Unfortunately the remaining two matrices, $\boldsymbol{C}_1$ and $\boldsymbol{D}_{12}$, have less apparent physical meaning. Their significance can be explained by examining the l_2 norm of the output z of the system S_o in Eq. (1),

$$\|z\|^2 = \sum_{t=0}^{\infty} \boldsymbol{x}(t)^T \boldsymbol{C}_1(t)^T \boldsymbol{C}_1(t)\boldsymbol{x}(t) + \boldsymbol{u}(t)^T \boldsymbol{D}_{12}(t)^T \boldsymbol{D}_{12}(t)\boldsymbol{u}(t) + 2\boldsymbol{x}(t)^T \boldsymbol{C}_1(t)^T \boldsymbol{D}_{12}(t)\boldsymbol{u}(t) \tag{21}$$

It follows from Eq. (21) that, similarly to standard linear quadratic control, the matrix function $\boldsymbol{C}_1$ places the weighting on the state, whereas $\boldsymbol{D}_{12}$ sets the focus on the control.

V. Magnetically Actuated Spacecraft

The objective of this section is to synthesize a three-axis attitude controller of a spacecraft in a low, highly inclined Earth orbit. The spacecraft is actuated by three mutually perpendicular electromagnetic coils. The interaction between the geomagnetic field and the magnetic field in the coils produces the control torque.

The satellite considered in this study is modeled as a rigid body in the Earth gravitational field influenced by the control torque generated by the magnetorquers. The orientation of the spacecraft principal coordinate system is related to the local-vertical–local-horizontal (LVLH) frame. The LVLH is a right orthogonal coordinate system with the origin at the spacecraft's center of mass. The z axis (local vertical) is parallel to the radius vector and points from the spacecraft center of mass to the center of the Earth. The positive y axis is pointed in the direction of the negative angular momentum vector of the orbit. The x axis (local horizontal) completes the right orthogonal coordinate system. The attitude is globally parameterized by the unit quaternion.[32,33] It is often advantageous for the attitude control synthesis to use a geometrical interpretation of a unit quaternion as a three-sphere $S^3 = \{\boldsymbol{q} \in \mathbb{R}^4 : \boldsymbol{q}^T\boldsymbol{q} = 1\}$.

The control torque $\boldsymbol{N}_{\text{ctrl}}$ of the magnetically actuated satellite always lies perpendicular to the geomagnetic field vector $\boldsymbol{b}$. Furthermore, a magnetic moment m generated in the direction parallel to the local geomagnetic field has no influence on the satellite motion. This can be explained by the following equality:

$$\boldsymbol{N}_{\text{ctrl}} = (\boldsymbol{m}_{\parallel} + \boldsymbol{m}_{\perp}) \times \boldsymbol{b} = \boldsymbol{m}_{\perp} \times \boldsymbol{b} \tag{22}$$

where $m_{\parallel}$ is the component of the magnetic moment parallel to $\boldsymbol{b}$, whereas $m_{\perp}$ is perpendicular to the local geomagnetic field. In conclusion, the necessary condition for power optimality of a control law is that the magnetic moment lies on a plane perpendicular to the geomagnetic field vector.

Consider the following mapping:

$$\tilde{\boldsymbol{m}} \mapsto \boldsymbol{m} : \boldsymbol{m} = \tilde{\boldsymbol{m}} \times \boldsymbol{b}/|\boldsymbol{b}|^2 \tag{23}$$

A new control signal for the satellite is denoted by $\tilde{\boldsymbol{m}}$. Now, the magnetic moment $\boldsymbol{m}$ is exactly perpendicular to the local geomagnetic field vector, and the control theory for a system with unconstrained input $\tilde{\boldsymbol{m}}$ can be applied. The direction of the vector $\tilde{\boldsymbol{m}}$ (contrary to $\boldsymbol{m}$) can be chosen arbitrarily by the controller.

The continuous time-linear model of the satellite motion is given in terms of the angular velocity of the spacecraft relative to the LVLH and the vector part of the attitude quaternion. The vector part of the quaternion $\boldsymbol{q} = [q_0,\ q_1,\ q_2,\ q_3]^T \in S^3$ is $\boldsymbol{\delta\tilde{q}} = [q_1\ q_2\ q_3]^T$. The components of $\boldsymbol{\delta\tilde{q}}$ can be considered as the coordinates in the local chart $\phi : U \to \mathbb{R}^3, \boldsymbol{q} \mapsto \boldsymbol{\delta\tilde{q}}$ of the open set $U = \{q \in S^3 : q_0 > 0\}$ onto the open ball $\{\boldsymbol{\delta\tilde{q}} \in \mathbb{R}^3 : \boldsymbol{\delta\tilde{q}}^T\boldsymbol{\delta\tilde{q}} < 1\}$. The continuous time state-space model of a low Earth orbit spacecraft[8] is

$$\frac{\mathrm{d}}{\mathrm{d}t}\begin{bmatrix}\boldsymbol{\delta\Omega}\\ \boldsymbol{\delta\tilde{q}}\end{bmatrix} = \boldsymbol{A}_s\begin{bmatrix}\boldsymbol{\delta\Omega}\\ \boldsymbol{\delta\tilde{q}}\end{bmatrix} + \boldsymbol{B}_s(t)\tilde{\boldsymbol{m}} \tag{24}$$

where

$$\boldsymbol{A}_s = \begin{bmatrix} 0 & 0 & -\sigma_x\omega_o & -6\omega_o^2\sigma_x & 0 & 0\\ 0 & 0 & 0 & 0 & 6\omega_o^2\sigma_y & 0\\ -\omega_o\sigma_z & 0 & 0 & 0 & 0 & 0\\ \frac{1}{2} & 0 & 0 & 0 & 0 & -\omega_o\\ 0 & \frac{1}{2} & 0 & 0 & 0 & 0\\ 0 & 0 & \frac{1}{2} & \omega_o & 0 & 0 \end{bmatrix}$$

$$\sigma_x = \frac{J_y - J_z}{J_x}, \qquad \sigma_y = \frac{J_z - J_x}{J_y}, \qquad \sigma_z = \frac{J_x - J_y}{J_z}$$

$$\boldsymbol{B}_s(t) = \begin{bmatrix} \dfrac{\boldsymbol{J}^{-1}}{|\boldsymbol{b}|^2}\begin{bmatrix} -b_y^2(t) - b_z^2(t) & b_x(t)b_y(t) & b_x(t)b_z(t)\\ b_x(t)b_y(t) & -b_x(t)^2 - b_z(t)^2 & b_y(t)b_z(t)\\ b_x(t)b_z(t) & b_y(t)b_z(t) & -b_x(t)^2 - b_y(t)^2 \end{bmatrix}\\ \begin{bmatrix} 0 & 0 & 0\\ 0 & 0 & 0\\ 0 & 0 & 0\end{bmatrix} \end{bmatrix}$$

and where ω_o is the orbital rate and J_x, J_y, and J_z are mean components on the diagonal of the inertia tensor $\boldsymbol{J}$, the principal moments of inertia. The matrix $\boldsymbol{B}_s(t)$ comes from the double cross product operation $-\boldsymbol{b}(t) \times (\boldsymbol{b}(t)\times)$. The upper left 3 by 3 submatrix of $\boldsymbol{A}_s$ is due to Euler coupling, the submatrix in the upper right corner arises from the gravity gradient, and the lower part of the matrix $\boldsymbol{A}$ is the linearized kinematics. Note that the orbit coordinate system used in Ref. 8 differs from LVLH employed in this paper. The y and z axes are reversed in direction. Therefore, there is a sign discrepancy in matrix $\boldsymbol{A}_s$ when Eq. (24) is compared with the previous model.[8]

VI. Simulation Results

To make a comparison with one of the authors' earlier results on the magnetic attitude control,[8] the same spacecraft has been chosen for simulation. It corresponds to the Danishørsted satellite launched in February 1999. The main body measures 0.34 by 0.45 by 0.72 m and is endowed with an 8-m-long instrument boom. The spacecraft is equipped with three mutually perpendicular coils producing up to 20 $\mathrm{A \cdot m^2}$. Additionally, it has a flux-gate magnetometer and a star camera for attitude determination. The moments of inertia used in the simulation study are 177.8 and 178.0 $\mathrm{kg \cdot m^2}$ and 1.3 $\mathrm{kg \cdot m^2}$ along the boom axis. The spacecraft is in 650 by 800 km elliptic orbit with an inclination of 96 deg. The spacecraft orbit is predicted by the SGP-4 (Simplified General Perturbations, Version 4), orbital model, and the magnetic field is simulated using a sixth-order IGRF (International Geomagnetic Reference Field) model.

The algorithm has been implemented in the MATLAB® LMI toolbox. Because the geomagnetic field is only approximately periodic, a periodic counterpart of the magnetic field of the Earth has been calculated[8] (Fig. 1).

The gain has been computed off-line and parameterized by the mean anomaly. The concept of synchronization is the same as for the periodic optimal contol.[8] The control gain is updated every 60, whereas the sampling time of the state is 10.

The rules for choosing the system matrices $\boldsymbol{B}_1$, $\boldsymbol{C}_1$, and $\boldsymbol{D}_{12}$ in the algorithm are as outlined at the end of Sec. IV. The ratio between

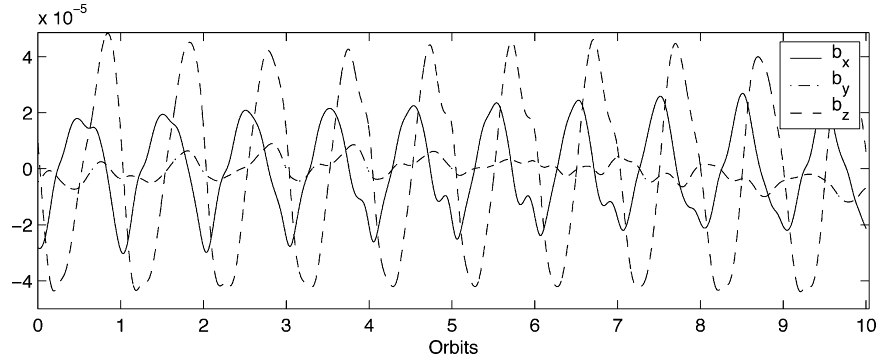

a) Geomagnetic field (tesla)

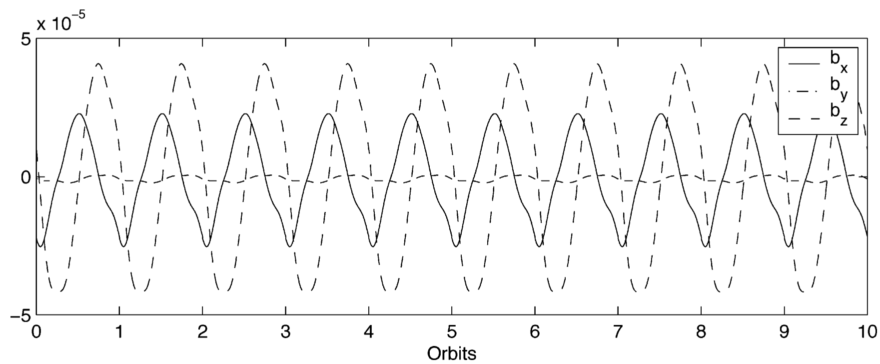

b) Averaged geomagnetic field (tesla)

Fig. 1 Geomagnetic field and its average in LVLH.

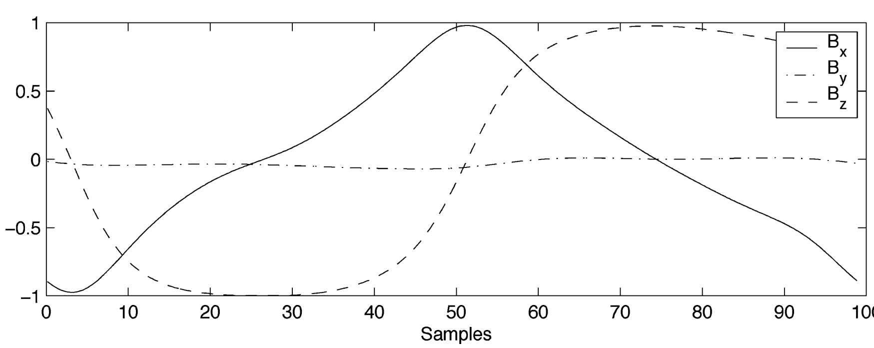

a) Normalized Earth magnetic field vector

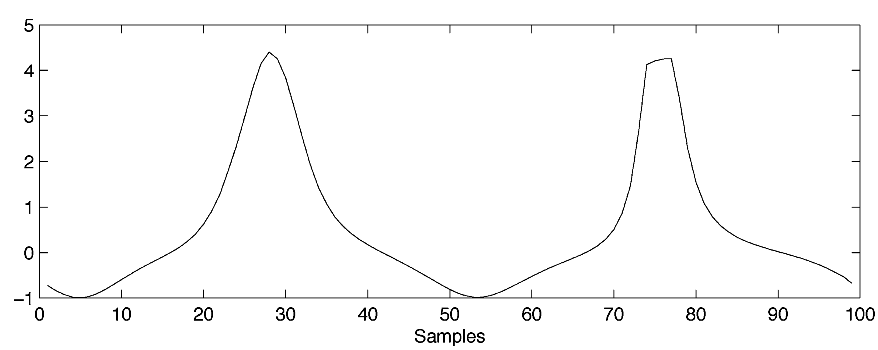

b) Roll-to-roll gain

Fig. 2 For single orbit, (1, 4) entry of gain matrix $K(t)$; roll-to-roll gain increase in polar regions.

$\boldsymbol{B}_1$ and $\boldsymbol{C}_1$ corresponds to proportion the of the disturbances to the desired accuracy in the state. Because the disturbance torque is expected not to exceed 10^{-4} N · m, the angular velocity will be below 10^{-3} rad/s and the attitude less than 10^{-2} rad, the H_2 performance is specified by the following matrices:

$$\boldsymbol{B}_1 = \begin{bmatrix} 0.01\boldsymbol{I} \\ 0 \end{bmatrix}, \qquad \boldsymbol{C}_1 = \begin{bmatrix} \boldsymbol{I} & 0 \\ 0 & 0.1\boldsymbol{I} \end{bmatrix}, \qquad \boldsymbol{D}_{12} = \begin{bmatrix} \boldsymbol{I} \\ \boldsymbol{I} \end{bmatrix} \tag{25}$$

The preceding weight matrices are spelled out with the accuracy of an order of magnitude. Their fine tuning, similar to the techniques employed in linear quadratic regulator design, is still possible. The eigenvalues of the monodromy matrix[16] are $(-0.17, 0.12, -0.01i, 0.01i, 0.00, 0.00)$, which indicates stability of the closed-loop system.

The resultant control gain is shown in Fig. 2. It is seen that near the polar zones, where the z component of the geomagnetic field vector

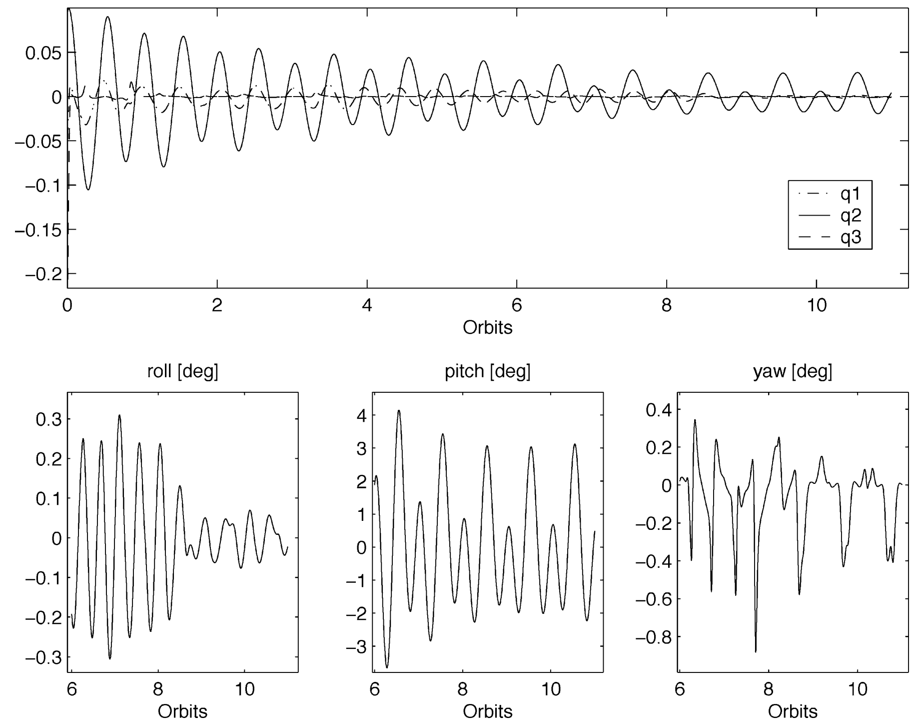

Fig. 3 Periodic H_2 control of the Ørsted satellite influenced by the aerodynamic drag; initial attitude 10 deg pitch, −15 deg roll, and −30 deg yaw.

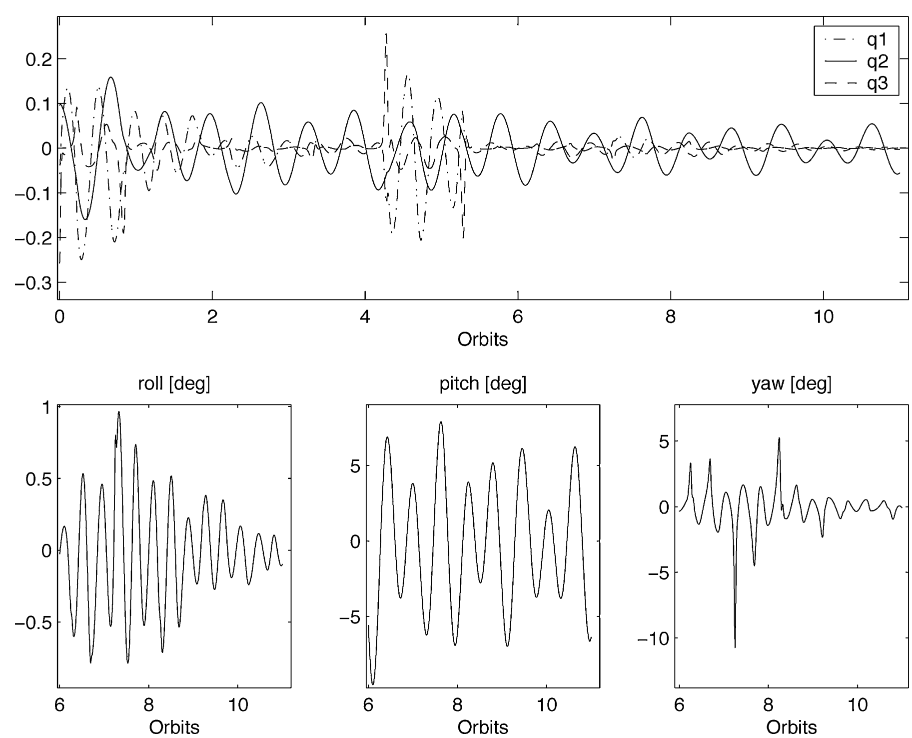

Fig. 4 Moments of inertia altered 22%; interval between fourth and sixth orbit show signs of instability.

reaches extremals, the periodic roll-to-roll gain $\boldsymbol{K}(1, 4)$ increases as expected.

A performance test for the H_2 attitude controller is shown in Fig. 3. The initial values for the simulation correspond to Ref. 8: Pitch is 10 deg, roll −15 deg, and yaw −30 deg. It is seen that the steady-state error of roll and yaw is less than 1 deg. Pitch is more difficult to control due to influence of the aerodynamic drag in this direction. It is kept on a level below 3 deg. This gives comparable results with the infinite and finite horizon control.[8]

There were no concerns regarding robustness in the development of the periodic H_2 control in Sec. IV. However, it is known from the time-invariant case[34] that the H_2 control method possesses intrinsic robustness properties. Figure 4 shows them; the moments of inertia are changed 22%. The steady-state accuracy of the attitude is below 10 deg. However, between the fourth and sixth orbit some signs of instability are already visible.

The simulation study has given rise to an observation that the computational burden of the suggested method is considerable. In the example above 2.8×10^6 floating point operations were used to compute the control gain. However, this is slightly less than 3.4×10^6 floating points operations used by the infinite and the finite horizon control. The onboard implementation is relatively simple; at each sampling time, it calculates a product of the magnetic field, the periodic gain $\boldsymbol{K}(t)$, and the state,

$$\boldsymbol{m}(t) = \boldsymbol{K}(t)\begin{bmatrix}\delta\boldsymbol{\Omega}(t)\\ \delta\tilde{\boldsymbol{q}}(t)\end{bmatrix} \times \frac{\boldsymbol{b}(t)}{|\boldsymbol{b}(t)|^2} \tag{26}$$

VII. Conclusions

This paper addressed the generalized H_2 suboptimal control synthesis for a magnetically actuated spacecraft. First, a relation between H_2 performance specification and the solution to a certain periodic Lyapunov equation were developed. Then, the necessary and sufficient conditions for solvability of the periodic H_2 control synthesis problem were formulated. The main contribution of the work is the design algorithm formulated as a set of LMI. The algorithm was implemented for the three-axis attitude control of the Ørsted spacecraft. The simulation study showed that the performance of the H_2 controller was similar to the periodic infinite and finite horizon controls.

Appendix: Proof of Theorem 2

The foremost component of the proof of Theorem 2 is the projection lemma.[28]

Lemma 1 (projection lemma): For arbitrary matrices $\boldsymbol{\Psi}_a$ and $\boldsymbol{\Psi}_b$ and a symmetric $\boldsymbol{P}$, the LMI

$$\boldsymbol{\Psi}_a^T \boldsymbol{X}\boldsymbol{\Psi}_b + \boldsymbol{\Psi}_b^T \boldsymbol{X}\boldsymbol{\Psi}_a + \boldsymbol{P} < 0 \tag{A1}$$

is solvable if and only if

$$\boldsymbol{W}_a^T \boldsymbol{P}\boldsymbol{W}_a < 0, \qquad \boldsymbol{W}_b^T \boldsymbol{P}\boldsymbol{W}_b < 0 \tag{A2}$$

where $\boldsymbol{W}_a$, and $\boldsymbol{W}_b$ are any matrices with columns forming bases for the null spaces of $\boldsymbol{\Psi}_a$ and $\boldsymbol{\Psi}_b$.

Proof of Theorem 1: From Eq. (15), the statement $\|s_c\|_2 < \gamma$ is equivalent to

$$\operatorname{tr}\sum_{t=0}^{N-1} \boldsymbol{B}_1(t)^T \boldsymbol{Q}^{-1}(t)\boldsymbol{B}_1(t) < N\gamma^2 \tag{A3}$$

where $\boldsymbol{Q}$ is N periodic and satisfies the inequality

$$\boldsymbol{Q}^{-1}(t-1) - \boldsymbol{A}_c(t)^T\boldsymbol{Q}^{-1}(t)\boldsymbol{A}_c(t) - \boldsymbol{C}_c(t)^T\boldsymbol{C}_c(t) > 0 \tag{A4}$$

but Eq. (A3) is equivalent to

$$\operatorname{tr}\left[\sum_{t=0}^{N-1}\boldsymbol{Z}(t)\right] < N\gamma^2 \tag{A5}$$

where $\boldsymbol{Z}(t)$ is a solution of the following LMI:

$$\boldsymbol{B}_1(t)^T\boldsymbol{Q}^{-1}(t)\boldsymbol{B}_1(t) < \boldsymbol{Z} \tag{A6}$$

The result of applying the Schur complement (see Ref. 28) on Eq. (A6) is the LMI (18).

The next step is to use the Schur complement twice in Eq. (A4), which gives two equivalent forms,

$$\begin{bmatrix}-\boldsymbol{Q}^{-1}(t-1) + \boldsymbol{A}_c(t)^T\boldsymbol{Q}^{-1}(t)\boldsymbol{A}_c(t) & \boldsymbol{C}_c(t)^T\\ \boldsymbol{C}_c(t) & -\boldsymbol{I}\end{bmatrix} < 0 \tag{A7}$$

$$\Updownarrow$$

$$\begin{bmatrix}-\boldsymbol{Q}(t) & \boldsymbol{A}_c(t) & 0\\ \boldsymbol{A}_c(t)^T & -\boldsymbol{Q}^{-1}(t-1) & \boldsymbol{C}_c(t)^T\\ 0 & \boldsymbol{C}_c(t) & -\boldsymbol{I}\end{bmatrix} < 0 \tag{A8}$$

For the control synthesis, Eq. (A8) is grouped into two terms: dependent on $\boldsymbol{K}(t)$ and on $\boldsymbol{Q}(t)$,

$$\begin{bmatrix}-\boldsymbol{Q}(t) & \boldsymbol{A}(t) & 0\\ \boldsymbol{A}(t)^T & -\boldsymbol{Q}^{-1}(t-1) & \boldsymbol{C}_1(t)^T\\ 0 & \boldsymbol{C}_1(t) & -\boldsymbol{I}\end{bmatrix}$$
$$+\left[\boldsymbol{B}_2(t)^T \quad 0 \quad \boldsymbol{D}_{12}(t)^T\right]^T\boldsymbol{K}(t)\left[0 \quad \boldsymbol{I} \quad 0\right]$$
$$+[0 \quad \boldsymbol{I} \quad 0]^T\boldsymbol{K}(t)^T\left[\boldsymbol{B}_2(t)^T \quad 0 \quad \boldsymbol{D}_{12}(t)^T\right] < 0 \tag{A9}$$

but the structure of Eq. (A9) corresponds to Eq. (A1); thus the LMI (A9) is solvable if and only if

$$\boldsymbol{W}_a(t)^T\begin{bmatrix}-\boldsymbol{Q}(t) & \boldsymbol{A}(t) & 0\\ \boldsymbol{A}(t)^T & -\boldsymbol{Q}^{-1}(t-1) & \boldsymbol{C}_1(t)^T\\ 0 & \boldsymbol{C}_1(t) & -\boldsymbol{I}\end{bmatrix}\boldsymbol{W}_a(t) < 0 \tag{A10}$$

$$\boldsymbol{W}_b(t)^T\begin{bmatrix}-\boldsymbol{Q}(t) & \boldsymbol{A}(t) & 0\\ \boldsymbol{A}(t)^T & -\boldsymbol{Q}^{-1}(t-1) & \boldsymbol{C}_1(t)^T\\ 0 & \boldsymbol{C}_1(t) & -\boldsymbol{I}\end{bmatrix}\boldsymbol{W}_b(t) < 0 \tag{A11}$$

where

$$\boldsymbol{W}_a(t) = \begin{bmatrix}\boldsymbol{W}_1(t) & 0\\ 0 & \boldsymbol{I}\\ \boldsymbol{W}_2(t) & 0\end{bmatrix} \quad \boldsymbol{W}_b(t) = \begin{bmatrix}\boldsymbol{I} & 0\\ 0 & 0\\ 0 & \boldsymbol{I}\end{bmatrix} \tag{A12}$$

The LMI (A11) is always fulfilled, whereas Eq. (A10) is equivalent to

$$\begin{bmatrix}-\boldsymbol{W}_1(t)^T\boldsymbol{Q}(t)\boldsymbol{W}_1(t) - \boldsymbol{W}_2(t)^T\boldsymbol{W}_2(t) & \boldsymbol{W}_1(t)^T\boldsymbol{A} + \boldsymbol{W}_2(t)^T\boldsymbol{C}_1(t)\\ \boldsymbol{A}(t)^T\boldsymbol{W}_1(t) + \boldsymbol{C}_1(t)^T\boldsymbol{W}_2(t) & -\boldsymbol{Q}^{-1}(t-1)\end{bmatrix}$$
$$< 0 \tag{A13}$$

When the Schur complement is applied to Eq. (A13), the LMI (17) is the result.

References

[1] Camillo, P., and Markley, F., "Orbit-Averaged Behavior of Magnetic Control Laws for Momentum Unloading," *Journal of Guidance and Control*, Vol. 3, No. 6, 1980, pp. 563–568.

[2] Hablani, H., "Comparative Stability Analyses and Performance of Magnetic Controllers for Momentum Bias Satellites," *Journal of Guidance, Control, and Dynamics*, Vol. 18, No. 6, 1995, pp. 1313–1320.

[3] Hablani, H., "Pole-Placement Technique for Magnetic Momentum Removal of Earth-Pointing Spacecraft," *Journal of Guidance, Control, and Dynamics*, Vol. 20, No. 2, 1997, pp. 268–275.

[4] Martel, F., Parimal, K., and Psiaki, M., "Active Magnetic Control System for Gravity Gradient Stabilized Spacecraft," *Annual AIAA/Utah State University Conference on Small Satellites*, AIAA, Washington, DC, 1988, pp. 1–10.

[5] Cavallo, A., Maria, G. D., Ferrara, F., and Nistri, P., "A Sliding Manifold Approach to Satellite Attitude Control," *12th IFAC World Congress*, Pergamon, New York, 1993, pp. 177–184.

[6] Arduini, C., and Baiocco, P., "Active Magnetic Damping Attitude Control for Gravity Gradient Stabilized Spacecraft," *Journal of Guidance, Control, and Dynamics*, Vol. 20, No. 1, 1997, pp. 117–122.

[7] Wisniewski, R., and Markley, F., "Optimal Magnetic Attitude Control," *14th IFAC World Congress*, Elsevier, New York, 1999.

[8] Wisniewski, R., "Linear Time-Varying Approach to Satellite Attitude Control Using Only Electromagnetic Actuation," *Journal of Guidance, Control, and Dynamics*, Vol. 23, No. 4, 2000, pp. 640–647.

[9] Psiaki, M., "Magnetic Torquer Attitude Control via Asymptotic Periodic Linear Quadratic Regulation," *Journal of Guidance, Control, and Dynamics*, Vol. 24, No. 2, 2001, pp. 386–394.

[10] Steyn, W., "Comparison of Low-Earth Orbitting Satellite Attitude Controllers Submitted to Controllability Constraints," *Journal of Guidance, Control, and Dynamics*, Vol. 17, No. 4, 1994, pp. 795–804.

[11] Wisniewski, R., and Blanke, M., "Three-Axis Satellite Attitude Control Based on Magnetic Torquing," *13th IFAC World Congress*, Pergamon, New York, 1996, pp. 291–297.

[12] Tabuada, P., Alves, P., Tavares, P., and Lima, P., "A Predictive Algorithm for Attitude Stabilization and Spin Control of Small Satellites," *European Control Conference*, Springer-Verlag, Berlin, 1999.

[13]Lovera, M., and Astolfi, A., "Global Attitude Regulation Using Magnetic Control," *40th Conference on Decision and Control*, IEEE Press, New York, 2001, pp. 4604–4609.

[14]Brockett, R., *Finite Dimensional Linear Systems*, Wiley, 1970.

[15]Bittanti, S., Colaneri, P., and De Nicolao, G., "The Periodic Riccati Equation," *The Riccati Equation*, edited by S. Bittanti, J. A. Laub, and J.-C. Willems, Springer-Verlag, 1991, pp. 127–162.

[16]Mohler, R., *Nonlinear Systems*, Dynamics and Control Vol., Prentice–Hall, Upper Saddle River, NJ, 1991.

[17]Bolzern, P., and Colaneri, P., "Inertia Theorems for Periodic Lyapunov Difference Equation and Periodic Riccati Equation," *Linear Algebra and Its Applications*, Vol. 85, Jan. 1987, pp. 249–265.

[18]Bittanti, S., and Nicolao, G. D., "The Difference Periodic Riccati Equation for the Periodic Prediction Problem," *IEEE Transactions on Automatic Control*, Vol. 33, No. 8, 1994, pp. 706–712.

[19]Khargonekar, P., Poolla, K., and Tannenbaum, A., "Robust Control of Linear Time-Invariant Plants Using Periodic Compensation," *IEEE Transactions on Automatic Control*, Vol. 30, No. 11, 1985, pp. 1088–1096.

[20]Colaneri, P., "Output Stabilization via Pole Placement of Discrete-Time Linear Periodic Systems," *IEEE Transactions on Automatic Control*, Vol. 36, No. 6, 1991, pp. 739–742.

[21]Colaneri, P., and Souza, C. D., "The H_∞ Control Problem for Continuous-Time Linear Periodic Systems," *2nd IFAC Workshop on System Structure and Control*, International Federation of Automatic Control, Laxenburg, Austria, 1992, pp. 292–296.

[22]Bittanti, S., and Colaneri, P., "An LMI Characterization of the Class of Stabilizing Controllers for Periodic Discrete-Time Systems," *14th International Federation of Automatic Control World Congress*, Elsevier, New York, 1999.

[23]Souza, C. E. D., and Trofino, A., "An LMI Approach to Stabilization of Linear Discrete-Time Periodic Systems," *International Journal of Control*, Vol. 73, No. 8, 2000, pp. 698–703.

[24]Dullerud, G., and Lall, S., "A New Approach for Analysis and Synthesis of Time-Varying Systems," *IEEE Transactions on Automatic Control*, Vol. 44, No. 8, 1999, pp. 1486–1497.

[25]Bamieh, B., and Pearson, J., "The H_2 Problem for Sampled Data Systems," *Systems and Control Letters*, Vol. 19, No. 1, 1992, pp. 1–12.

[26]Gahinet, P., and Apkarian, P., "A Linear Matrix Inequality Approach to H_∞ Control," *International Journal of Robust and Nonlinear Control*, Vol. 4, No. 4, 1991, pp. 421–448.

[27]Boyd, S., Ghaouri, L. E., Feron, E., and Balakrishnan, V., *Linear Matrix Inequality in System and Control Theory*, Society for Industrial and Applied Mathematics, Philadelphia, 1994.

[28]Scherer, C., and Weiland, S., *Linear Matrix Inequality in Control*, Lecture Notes DISC Course, Technishe Universiteit Delft, The Netherlands, 1999.

[29]Da Prato, G., and Ichikawa, A., "Quadratic Control for Linear Periodic Systems," *Applied Mathematics and Optimization*, Vol. 18, No. 1, 1988, pp. 39–66.

[30]Halanay, A., and Ionescu, V., *Time-Varying Discrete Linear Systems*, Birkhauser Verlag, 1970.

[31]Nagy, B., and Foias, C., *Harmonic Analysis of Operators on Hilbert Space*, Elsevier, New York, 1970.

[32]Goldstein, H., *Classical Mechanics*, Addison Wesley Longman, Reading, MA, 1980.

[33]Wertz, J., *Spacecraft Attitude Determination and Control*, Kluwer Academic, Norwell, MA, 1990.

[34]Zhou, K., Doyle, J., and Glover, K., *Robust and Optimal Control*, Prentice–Hall, Upper Saddle River, NJ, 1996.